Biointerface Research in Applied Chemistry
Platinum Open Access Journal (ISSN: 2069-5837)

Article
Volume 12, Issue 4, 2022, 5716 - 5726
https://doi.org/10.33263/BRIAC124.57165726

Comparison of Anticancer Effects of Carvone, Carvone-Rich Essential Oils, and Chitosan Nanoparticles Containing Each of Them

Hiva Alipanah [1], Fatemeh Rasti [2], Elham Zarenezhad [2], Azizallah Dehghan [2], Barsa Sahebnazar [2], Mahmoud Osanloo [3,*]

[1] Department of Physiology, School of Medicine, Fasa University of Medical Sciences, Fasa, Iran; alipanah.hiwa@yahoo.com (H.A.);
[2] Noncommunicable Diseases Research Center, Fasa University of Medical Sciences, Fasa, Iran; fatemehrasti79@gmail.com (F.R.); el.zarenezhad@gmail.com (E.Z.); dehghanaz@gmail.com (A.D.); sahebnazarbarsa@gmail.com (B.S.);
[3] Department of Medical Nanotechnology, School of Advanced Technologies in Medicine, Fasa University of Medical Sciences, Fasa, Iran; m.osanloo@fums.ac.ir (M.O);
* Correspondence: m.osanloo@fums.ac.ir, osanloo_mahmood@yahoo.com (M.O.);

Scopus Author ID 57192379172

Received: 31.08.2021; Revised: 10.10.2021; Accepted: 12.10.2021; Published: 21.10.2021

Abstract: Cancers were the first cause of death in 2020; breast and skin are two common cancers worldwide. The most common cancer treatment approach is still chemotherapy; however, as side effects and multidrug resistance, the development of green nano drugs has received much attention. In this study, the chemical composition of *Mentha spicata* and *Tanacetum balsamita* essential oils was first investigated. The anticancer effects of them and carvone (as their major ingredients) were then evaluated on human melanoma (A375) and breast cancer (MDA-MB468) cells. After that, an attempt was made to improve their efficacies by preparing chitosan nanoparticles containing each of them. The efficacies of nanoformulations showed a significant improvement ($p < 0.05$) compared to their non-formulated states. The best-observed potency was related to chitosan nanoparticles containing *T. balsamita* essential oil with a particle size of 195 ± 7 nm; IC_{50} values against A375 and MDA-MB468 were observed at 85.3 and 240.1 µg/mL. Thus, the nanoformulation with green ingredients could be considered a proper candidate for further consideration *in vivo* studies.

Keywords: *Mentha spicata*; *Tanacetum balsamita*; melanoma; breast cancer

1. Introduction

Cancer with around 10 million deaths is a leading cause of death worldwide in 2020 [1, 2]. Breast cancer with 2.26 million cases and skin cancer (non-melanoma and melanoma) with around 1.5 million are the first and fifth common types of cancer [3]. Besides, they caused 685000 and 121000 death only in 2020 [3, 4]. Despite the rising cancer rate, common treatment approaches like chemotherapy, surgery, and radiotherapy were underdeveloped; they also have side effects [5, 6]. Therefore, the development of new anticancer agents is crucial.

The use of plant-derived substances, especially essential oils (EOs), is a promising approach for bypassing the side effects of chemotherapy agents [7]. However, the efficacy of EOs is generally less than synthetic drugs. The preparation of nanostructures containing EOs (nanofibers, nanoparticles, and lipid nanocarriers) has thus been recently proposed as a

practical solution to improve their efficacies [8, 9]. Nowadays, chitosan nanoparticles, as a naturally biocompatible and biodegradable polymer, have been widely used in drug delivery studies [10, 11]. For instance, chitosan nanoparticles containing *Torreya grandis* EO with a particle size of 349.6 nm were proposed; it showed a more potent antibacterial agent than non-formulated EO [12]. In another research, *Carum copticum* EO was successfully loaded in chitosan nanoparticles with 30-80 nm diameter; the nanoparticles showed more antioxidant effect than EO [13].

Mentha spicata L. and *Tanacetum balsamita* L. are two important medicinal plants with a broad range of biological effects [7, 14]. For instance, *M. spicata* is used as a diuretic, antispasmodic, and anti-flatulent and controls respiratory and gastrointestinal ailments [15]. Some previous studies also reported antiproliferative effects of *M. spicata* on particular breast cancer cell lines (e.g., MCF7, Wehi-16, U937, and KB), fibrosarcoma, leukemic monocyte, and mouth epidermal carcinoma [16-19]. Moreover, anticancer effects (LD_{50}) of *M. spicata* EO against different human-derived tumor cell lines, including T47D, HCT116, and MCF7, were reported at 324, 279, and 975 (µg/mL) [20]. Also, *Bradaweel et al.* evaluated antiproliferative activities associated with the *M. spicata* against three human cancer cell lines (e.g., T47D, HCT116, and MCF7) [20]. In addition, many studies introduced clinical functions for *T. balsamita*, such as spasmolytic and diuretic roles [7]. Moreover, anti-inflammatory and analgesic effects of *T. balsamita* EO in a rat model were also reported [21]. Due to the medicinal properties of *T. balsamita* and *M. spicata* EOs, a new trend could develop anticancer agents using their major ingredients, i.e., carvone [14, 15]. From the literature, carvone as an active component could induce caspase-mediated cell death in breast cancer cells such as MCF7 and MDA-MB231, gastric cancer AGS cells, and colon cancer cells (HT29 and SW480) [22-24].

In the current study, the anticancer effects of carvone, *T. balsamita*, *M. spicata* were first investigated against a human melanoma cell line (A375) and a human breast cancer cell line (MDA-MB468). An attempt was then made to improve their efficacies by preparing chitosan nanoparticles containing each.

2. Materials and Methods

2.1.Materials.

MDA-MB468 (ATCC HTB132) and A375 (ATCC CRL1619) cell lines were obtained from the Pasteur Institute of Iran. Tripolyphosphate, chitosan low molecular weight (75-85% de-acetylation degree), carvone, and tween 20 were bought from Sigma-Aldrich (USA). *M. spicata* and *T. balsamita* EOs were purchased from Pharmaceutical Company Essential Oil Dr. Soleimani (Iran).

2.2. Chemical compositions of the Eos.

Ingredients of *M. spicata* and *T. balsamita* EOs were identified by a Gas Chromatograph as described in our previous study [25].

2.3. EOs or carvone chitosan nanoparticles preparation.

We used the ionic gelation to prepare chitosan nanoparticles containing carvone or EOs as described in our previous study with a slight modification [26]. In the beginning, chitosan

powder (0.25% w/v) was dissolved at 2000 rpm in acetic acid 1% (an aqueous solution) at ambient temperature. The solution was then centrifuged (30 min, 7000 rpm) to precipitate undissolved chitosan. Next, carvone, *M. spicata*, and *T. balsamita* EOs were dissolved (0.5% w/v) in the prepared chitosan solution containing tween 20 (0.5% w/v) separately; the obtained solutions were then stirred for 10 min at 2000 rpm. Finally, we added tripolyphosphate solution (0.15% w/w) using a syringe pump (1 mL/h) and stirred for 40 min. The prepared nanoformulations were abbreviated CVChiNPs, MSChiNPs, and TBChiNPs, and used for characterizations and MTT assays.

2.4. Size analyses.

The particle size of CVChiNPs, MSChiNPs, and TBChiNPs was investigated by Dynamic Light Scattering (DLS; 9900 series; K-One Nano Ltd; Korea). Particle size distribution (SPAN) of them were calculated using equation $D90 - D10/D50$. D is diameter, 90, 50, and 10 are a percentage of particles with lower diameters than these defined values.

2.5. Investigation loading of carvone, M. spicata, and T. balsamita EOs in chitosan nanoparticles.

Attenuated Total Reflection-Fourier Transform Infrared (ATR-FTIR) was used to characterize functional groups and confirm the samples' successful loading in the chitosan nanoparticles. Free chitosan nanoparticles, carvone, *M. spicata* EO, *T. balsamita* EO, and their nano-formulated states (CVChiNPs, MSChiNPs, and TBChiNPs) were subjected to ATR-FTIR instruments without any preparation process. Spectra were recorded (400–4000 cm^{-1}) using the device (Tensor II, Bruker, Germany).

2.6. MTT assay.

The anticancer effects of carvone, *M. spicata* EO, *T. balsamita* EO, CVChiNPs, MSChiNPs, and TBChiNPs were investigated using the MTT cell proliferation assay as described in our previous study [26]. Briefly, carvone, *M. spicata*, and *T. balsamita* were first dissolved in the phosphate-buffered saline solution with 0.5% (w/v) DMSO, equal to the as-prepared nanoformulations. Then, seeded cells (MDA-MB468 and A375) in 96-well culture plates containing 75 µL DMEM complete medium (10% FBS and 1% penicillin/streptomycin) were treated with different amounts of samples to reach concentrations of 1200, 600, 300, 150, and 75 µg/mL. After 24 hours of incubation, nanoformulations' milky color of wells were first washed with PBS, and 100 µL/well of MTT solution 0.5 µg/mL was then added. After 4 hours of incubation, 100 µL/well DMSO was added for formazan solubilization. Cell viability at different concentrations was calculated by comparing the optical density of control groups (no treated) and treated using at 570 nm.

3. Results

3.1. Constituents of M. spicata and T. balsamita Eos.

Identified compounds in *M. spicata* and *T. balsamita* EOs with a high portion than 1% are listed in Table 1; they comprised 90.6% of all identified components in *M. spicata* and 84.3% in *T. balsamita*. Besides, carvone was the major ingredient in both; 37.2 and 36.3 %.

Table 1. Chemical ingredients (> 1%) identified in the EOs by Gas Chromatography-Mass Spectrometry analysis.

Retention index	Compounds	*M. spicata*		*T. balsamita*	
		Area	%	Area	%
931	α-pinene	82848781	2.5	---	---
949	comphene	44325854	1.3	---	---
970	sabinene	63810507	1.9	---	---
976	β-pinene	110567647	3.4	---	---
1023	*p*-cymene	---	---	45489319	1.3
1025	1,8-cineole	---	---	67090832	2.0
1026	limonene	936146024	28.5	125222965	3.7
1101	α-thujone	---	---	90781085	2.7
1113	β-thujone	---	---	458741960	13.4
1121	*trans*-p-mentha-2,8-dien-1-ol	---	---	45749024	5.3
1159	iso-borneol	---	---	39407708	1.2
1168	borneol	130589576	4.0	---	---
1187	α-terpineol	66211461	2.0	---	---
1191	*cis*-dihydro carvone	---	---	61508804	1.9
1193	dihydrocarveol neo	88471507	2.7	---	---
1215	*trans*-carveol	---	---	39066428	1.1
1234	pulegone	108555599	3.3	---	---
1243	carvone	1221316667	37.2	1238470188	36.3
1342	piperitenone	87099203	2.7	---	---
1418	*trans*-caryophyllene	34507802	1.1	---	---
1480	Germacrene D	---	---	73253122	2.1
1493	zingiberene	---	---	46200785	1.4
1504	β-bisabolene	---	---	147778675	4.3
1522	δ-cadinene	---	---	55973474	1.6
1560	germacrene B	---	---	32966540	1.0
1641	tau-muurolol	---	---	53704860	1.6
1966	ilicic acid methyl ester	---	---	58607545	1.7
Total			90.6		84.3

3.2. Particle size and particle size distribution of CVChiNPs, MSChiNPs, and TBChiNPs.

DLS diagrams of CVChiNPs, MSChiNPs, and TBChiNPs with particle sizes of 217 ± 9, 161 ± 4, and 195 ± 7 nm are depicted in Figure 1. Their SPAN values were obtained as 0.89, 0.92, and 0.91; their narrow particle size distributions are confirmed since SPAN values are less than 1 [27]. In addition, the presence of a peak sharp in all three nanoformulations also indicates their narrow particle size distribution.

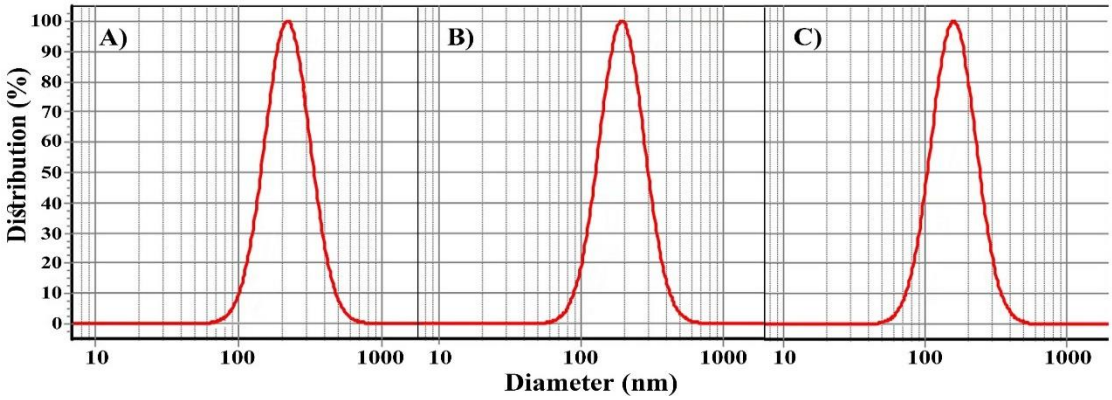

Figure 1. DLS diagrams of chitosan nanoparticles containing-carvone (A = 217 ± 9 nm), -*M. spicata* EO (B = 161 ± 4 nm), and -*T. balsamita* EO (C = 195 ± 7 nm).

3.3. Loading of carvone and EOs in chitosan nanoparticles.

In Figure 2A, the sharp peak at 1700 cm^{-1} attributed to C=O (stretching) could be related to the carbonyl group in tween and chitosan. The strong band at 1094 cm^{-1} corresponds to symmetric and anti-symmetric phosphodioxy (PO_2) structure, and the characteristic peak at

about 1020 cm^{-1} relates to anti-symmetric and symmetric stretching in the phosphite (PO_3) structure. In addition, two new peaks at 1280 and 1152 cm^{-1} have appeared after the crosslinking process. They belong to anti-symmetric stretching vibrations of PO_2 groups in tripolyphosphate ions; they confirm the ionic links between (NH_3^+) chitosan and anionic structure in tripolyphosphate [26]. The ATR-FTIR spectrum of pure carvone (Figure 2B) shows the band at 3083 cm^{-1} related to the stretching vibration of =C-H, and the bands at 2970, 2922, and 2886 cm^{-1} –CH stretching vibration. The characteristic band at 1668 cm^{-1} relates to stretching vibration of C=O, the peak at 1644 cm^{-1} corresponding to C=C stretching. Moreover, the peak at 1365 cm^{-1} relates to CH_3, and the band at 1109 cm^{-1} relates to C-O bending vibration. In Figure 2C, approximately most carvone characteristic bands are seen in the spectrum of CVChiNPs, similar to small wavenumber changes. Two strong peaks were shown at 1544 cm^{-1} (C-O-C) and 1281 cm^{-1} (amide II), which can be related to the complex preparation with electrostatic linking between (NH_3^+) structure of chitosan and phosphoric groups of tripolyphosphate within the chitosan nanoparticles [26].

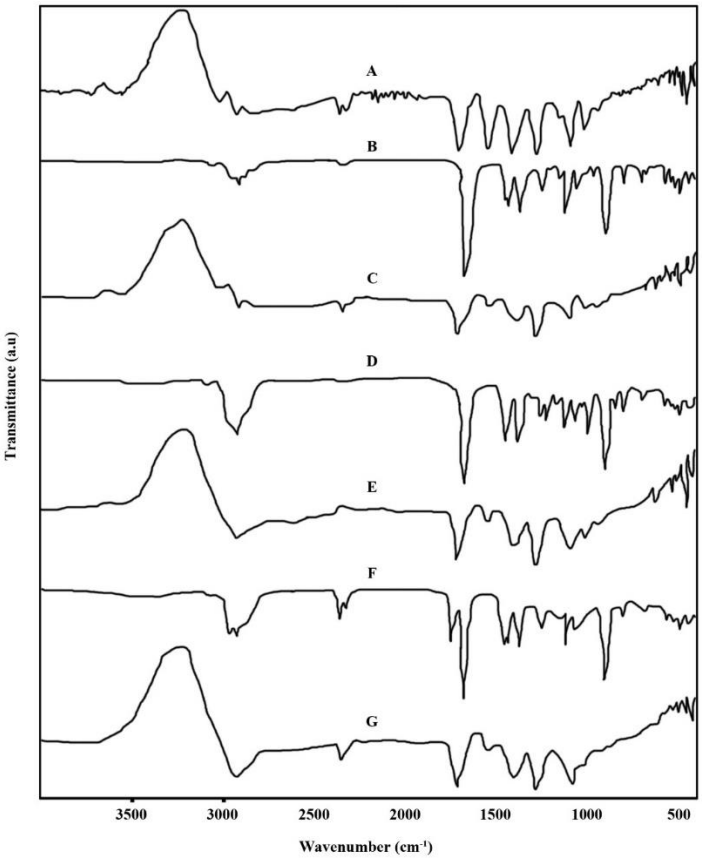

Figure 2. ATR-FTIR analyses of free chitosan nanoparticles (A), carvone (B), chitosan nanoparticles containing carvone (CVChiNPs) (C), *M. spicata* EO (D), chitosan nanoparticles containing *M. spicata* EO (MSChiNPs) (E), *T. balsamita* EO (F), and chitosan nanoparticles containing *T. balsamita* EO (TBChiNPs) (G).

In Figure 2D, the ATR-FTIR spectrum of pure *M. spicata* is displayed; the wideband at around 3462 cm^{-1} can be corresponding to hydroxyl groups, and the band at 3075 cm^{-1} attributed to =C-H (stretching vibration). The peaks at 2965 and 2922 cm^{-1} showed –CH stretching vibration, the sharp band at 1712 cm^{-1} corresponding to C=O, and the band at 1674 cm^{-1} is attributed to C=C stretching. The peak at 1373 cm^{-1} is related to CH_3, and the band at 1016 cm^{-1} relates to C-O bending vibration. In Figure 2E, the two strong bands at 1555 cm^{-1} (C-O-C) and 1230 cm^{-1} (amide II) can be related to the complex preparation between NH_3^+ groups chitosan and anionic structure tripolyphosphate. Furthermore, all the characteristic

peaks appear in the spectrum of *M. spicata* EO at the same wavenumber; the results indicate that the EO was successfully loaded in MSChiNPs.

The ATR-FTIR spectrum of pure *T. balsamita* EO is displayed in Figure 2F; the broad peak at about 3620 cm^{-1} can be corresponding to hydroxyl groups, and the peak at 3079 cm^{-1} is related to =C-H (stretching vibration). The peaks at 2958 and 2924 cm^{-1} demonstrated –CH stretching vibration, the peak at 1712 cm^{-1} can be attributed to C=O, and the band at 1645 cm^{-1} is related to C=C stretching. The band at 1366 cm^{-1} corresponded to CH_3, and the peak at 1110 cm^{-1} is attributed to C-O bending vibration. In Figure 2G, the ATR-FTIR spectrum of TBChiNPs showed a sharp band at 1280 cm^{-1} belonging to C-N stretching that confirmed the complex preparation whit linking electrostatic between NH_3^+ groups of chitosan and anionic groups of tripolyphosphate. The peak around 1543 cm^{-1} can correspond to C-N stretching and relates to the amide structure. All the other peaks appear in the spectrum of *T. balsamita* EO at the same wavenumber; it could be confirmed that the EO was encapsulated into TBChiNPs.

3.4. Anticancer effects of carvone, M. spicata EO, and T. balsamita EO versus chitosan nanoparticles containing them.

Anticancer effects of carvone, *M. spicata* EO, and *T. balsamita* EO versus chitosan nanoparticles containing them against A375 cells were observed in a dose-dependent manner (Figure 3). Interestingly, the viability of cells after treatment with CVChiNPs and TBChiNPs at three concentrations of 300, 600, and 1200 µg/mL were reduced to ≤ 15%. Moreover, nanoformulations at all concentrations indicated more anticancer effects than their non-formulated states ($p < 0.05$).

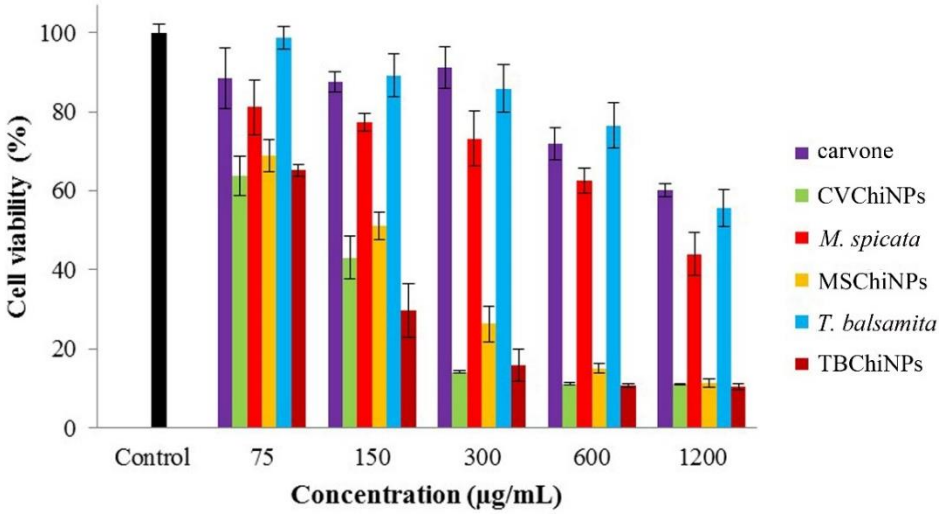

Figure 3. Anticancer effects of carvone, *M. spicata* EO, and *T. balsamita* EO versus chitosan nanoparticles containing them (CVChiNPs, MSChiNPs, and TBChiNPs) against A375 cells. Data are mean ± SD (n = 3).

Figure 4 indicated the dose-dependent effects of the samples on the MDA-MB468 cells line. However, this cell line showed less sensitivity to the samples than A375 cells; only at the highest concentration of nanoformulations (1200 µg/mL) was cell viability decreased to less than 10%. Moreover, *M. spicata* at three concentrations (75, 150, and 300 µg/mL) showed more potency than its nano-formulated states (MSChiNPs) ($p < 0.05$); however, at two highest concentrations (600, and 1200) efficacy of MSChiNPs was more potent ($p < 0.05$). In the other two samples, nanoformulations at four concentrations (150-1200 µg/mL) indicated significantly more anticancer effects than their non-formulated states ($p < 0.05$).

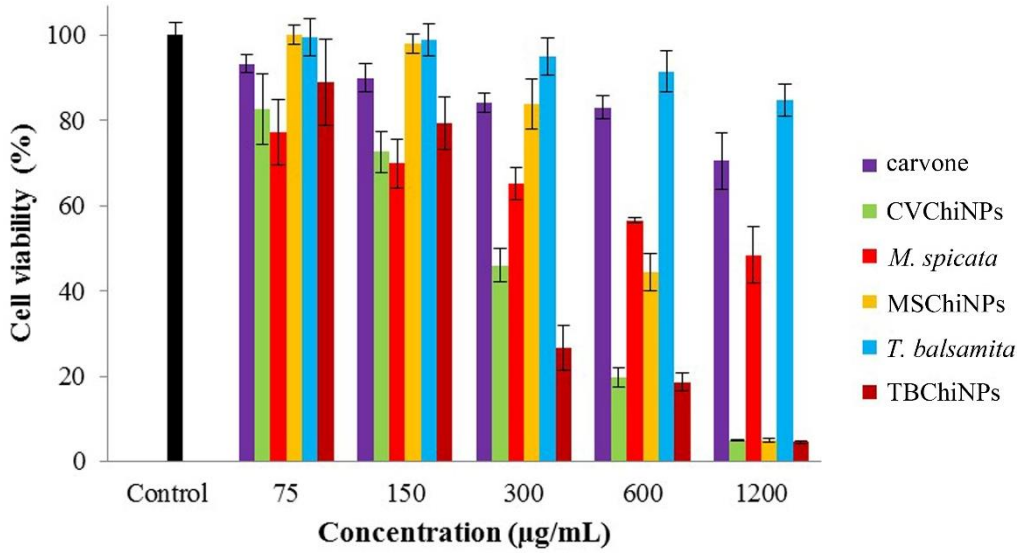

Figure 4. Anticancer effects of carvone, *M. spicata* EO, and *T. balsamita* EO versus chitosan nanoparticles containing them (CVChiNPs, MSChiNPs, and TBChiNPs) against MDA-MB468 cells. Data are mean ± SD (n = 3).

Anticancer effects (IC_{50}) of samples against A375 and MDA-MB468 cells are listed in Table 2. IC_{50} values of all nanoformulations against A375 and MDA-MB468 were significantly more potent than their non-formulated states ($p < 0.05$). Moreover, TBChiNPs with IC_{50} values of 85.3 and 240.1 µg/mL showed the best efficacy against both cell lines.

Table 2. Anticancer effects of carvone, *M. spicata EO*, and *T. balsamita* EO versus chitosan nanoparticles containing them (CVChiNPs, MSChiNPs, and TBChiNPs) against MDA-MB468 and A375 cells.

Cell lines	**A375**		**MDA-MB468**	
Samples	**IC_{50}[a]**		**IC_{50}**	
	LCL[b]	**UCL[c]**	**LCL**	**UCL**
carvone	3657.4		6038.0	
	448	29826	2931	12435
CVChiNPs	99.1		236.2	
	50	195	198	281
***M. spicata* EO**	1136.2		1067.7	
	675	1911	939	1213
MSChiNPs	143.4		514.6	
	112	182	466	567
***T. balsamita* EO**	1312.1		2323.6	
	687	2503	1007	5357
TBChiNPs	85.3		240.1	
	41	177	192	299

[a] Inhibitory Concentration 50% (µg/mL); [b] Lower Confidence Limit (95%); [c] Upper Confidence Limit (95%).

4. Discussions

In developing new drugs, preclinical models such as in vitro human cell lines should be first performed to find effective chemo-preventive/therapeutic agents [28-30]. The selection of the targeted cell line is also important. For example, as may be expected from genetic, morphologic, and phenotypic evidence, the A375 cell line is a more aggressive and metastatic cancer with poor chemotherapy responsiveness, which could be an effective evaluation model for anti-melanoma cancer agents [31, 32]. On the other hand, highly heterogeneous cancer such as the MDA-MB468 cell line is an in vitro cancer cell model without estrogen, progesterone, and HER2 receptors (a triple-negative breast cancer cell model). It is commonly used in research on proliferation, metastasis, migration, and chemical breast cancer treatments [33, 34]. Thus these two cell lines were used in the current study.

As listed in Table 1, the only component found in the *M. spicata* and *T. balsamita* EOs was carvone; it contained about 37% of both. The most important issue that is not yet well clarified is whether the biological potency of EOs is due to their main ingredient(s) or the whole oils as complex mixtures. From the literature, it seems that more potency of an EO or component strongly depends on the organism under study. For instance, IC_{50} values of clove EO against *Klebsiella pneumoniae*, *Pseudomonas aeruginosa*, and *Staphylococcus aureus* did not significantly differ with eugenol (its major ingredient); the difference against *Escherichia coli* was only significant. Moreover, no significant difference was observed between the effects of clove EO and eugenol against *Leishmania major* and *Leishmania tropica* [25]. Nevertheless, the current study results did not specify anything; both EOs and carvone against A375 cells were not significantly different together ($p > 0.05$): although the efficacy of EOs was relatively more potent than carvone. However, the results were quite different for MDA-MB468 cells. The IC_{50} value of *M. spicata* (1067 µg/mL) was more potent than *T. balsamita* (2323 µg/mL); however, this difference was not statistically significant ($p > 0.05$). Besides, *M. spicata* EO was significantly more potent ($p < 0.05$) than carvone (6038 µg/mL).

In the current study, an attempt was made to improve the anticancer effects of carvone, *T. balsamita*, and *M. spicata* EOs by preparing chitosan nanoparticles containing each of them. No report was found on preparing any nanoformulation of *T. balsamita* EO in the literature. However, some nanoformulation on *M. spicata* EO has been reported; its nanoemulsion with a droplet size of 97.8 nm was prepared as green larvicide against *Culex pipiens* and *Musca domestica* [35]. Furthermore, in a report, chitosan coating containing *M. spicata* EO was proposed as active packaging material with proper antibacterial against *Listeria monocytogenes* to preserve fresh strawberries [36]. Besides, such proposed coating also showed antibacterial effects against some species of *Pseudomonas* [37]. Furthermore, in another research, *M. spicata* extract as an antioxidant agent was successfully capsulated in chitosan nanoparticles [38]. Moreover, its aqueous extract was also used as a reducing agent for the green synthesis of silver nanoparticles (350–500 nm) [39].

The current study showed improvement in the efficacy of chitosan nanoparticles versus non-formulated states. For instance, the IC_{50} value of *M. spicata* 1136 µg/mL against A375 cells was decreased to 143 µg/mL in a nano-formulated state (MSChiNPs). The IC_{50} value of carvone against MDA-MB468, 6038 µg/mL, was dramatically decreased to 236 µg/mL in the nano-formulated state (CVChiNPs). Existing reports could justify these improvements; e.g., when drugs or EOs are dissolved in their proper solvents, obtained droplet size is around ≤ 2 nm [40,41]. When drugs or EOs are loaded in a nanocarrier with a particle size of ~ 200 nm (such as-prepared chitosan nanoparticles in the current study), about half a million droplets could be incorporated into a particle [42, 43]; so at lower concentrations compared to non-formulated could show higher efficacy [44, 45]. Besides, they could easily pass through larger gap junctions of cancer cells with a nanometer size than normal cells [46]. The large surface area and high surface energy of nanocarriers and intrinsic bioadhesive of chitosan nanoparticles also led to better interaction with cells [47, 48]. However, more investigations are recommended for comparing the mode of actions of non-formulated samples vs. their nano-formulated states.

5. Conclusions

At first, ingredients of EOs of *M. spicata* and *T. balsamita* EOs were identified using Gas Chromatography-Mass Spectrometry analysis. Their anticancer activity and carvone (their

major component) were then evaluated against human melanoma and breast cancer cells (MDA-MB468 and A375). Results demonstrated that *M. spicata*, *T. balsamita* EOs, and carvone could inhibit cell proliferation at all examined cells. After that, an attempt was made to improve their efficacy by preparing chitosan nanoparticles containing each. Chitosan nanoparticles containing *T. balsamita* EO with IC_{50} values of 85.3 and 240.1 µg/mL showed the best efficacy against both cell lines; it could thus be considered for further investigations such as *in vivo* or even supplementary medicine.

Funding

This study was funded by Fasa University of Medical Sciences, Fasa, Iran (grant number 400057). It has been ethically approved by the ethical committee; IR.FUMS.REC.1400.057.

Acknowledgments

Not applicable.

Conflicts of Interest

There is no conflict of interest amongst the authors.

References

1. World Health Organization. Cancer. https://www.who.int/health-topics/cancer#tab=tab_1.
2. Ferlay, J.; Ervik, M.; Lam, F.; Colombet, M.; Mery, L.; Piñeros, M.; Znaor, A.; Soerjomataram, I.; Bray, F. *Global cancer observatory: Cancer today* **2020**, Lyon, France: International Agency for Research on Cancer. Available from: https://gco.iarc.fr.
3. World Health Organization. Cancer. https://www.who.int/news-room/fact-sheets/detail/cancer.
4. Sung, H.; Ferlay, J.; Siegel, R.L.; Laversanne, M.; Soerjomataram, I.; Jemal, A.; Bray, F. Global cancer statistics 2020: GLOBOCAN estimates of incidence and mortality worldwide for 36 cancers in 185 countries. *CA Cancer J Clin* **2021**, *71*, 209-249, https://doi.org/10.3322/caac.21660.
5. Haider, T.; Pandey, V.; Banjare, N.; Gupta, P.N.; Soni, V. Drug resistance in cancer: mechanisms and tackling strategies. *Pharmacol. Rep.* **2020**, *72*, 1125–1151, https://doi.org/10.1007/s43440-020-00138-7.
6. Blowman, K.; Magalhães, M.; Lemos, M.; Cabral, C.; Pires, I. Anticancer properties of essential oils and other natural products. Evidence-based Complement. *Evid. Based Complement. Alternat. Med.* **2018**, *2018*, 3149362, https://doi.org/10.1155/2018/3149362.
7. Faraloni, C. Antioxidant Property and Antimicrobial Activity of the Aromatic Plant *Balsamita major* Desf. *International Journal of Clinical & Medical Microbiology* **2018**, *3*, 3:IJCMM-138, https://doi.org/10.15344/2456-4028/2018/138.
8. Osanloo, M.; Arish, J.; Sereshti, H. Developed methods for the preparation of electrospun nanofibers containing plant-derived oil or essential oil: a systematic review. *Polymer Bulletin* **2020**, *77*, 6085-6104, https://link.springer.com/article/10.1007/s00289-019-03042-0.
9. Esmaili, F.; Sanei-Dehkordi, A.; Amoozegar, F.; Osanloo, M. A Review on the Use of Essential Oil-Based Nanoformulations in Control of Mosquitoes. *Biointerface Research in Applied Chemistry* **2021**, *11*, 12516-12529, https://doi.org/10.33263/BRIAC115.1251612529.
10. Mohammed, M.A.; Syeda, J.T.M.; Wasan, K.M.; Wasan, E.K. An Overview of Chitosan Nanoparticles and Its Application in Non-Parenteral Drug Delivery. *Pharmaceutics* **2017**, *9*, 53, https://doi.org/10.3390/pharmaceutics9040053.
11. Zhang, X.; Yang, X.; Ji, J.; Liu, A.; Zhai, G. Tumor targeting strategies for chitosan-based nanoparticles. *Colloids and Surfaces B: Biointerfaces* **2016**, *148*, 460-473, https://doi.org/10.1016/j.colsurfb.2016.09.020.
12. Wu, J.; Shu, Q.; Niu, Y.; Jiao, Y.; Chen, Q. Preparation, Characterization, and Antibacterial Effects of Chitosan Nanoparticles Embedded with Essential Oils Synthesized in an Ionic Liquid Containing System. *J. Agric. Food Chem.* **2018**, *66*, 7006-7014, https://doi.org/10.1021/acs.jafc.8b01428.

13. Esmaeili, A.; Asgari, A. In vitro release and biological activities of *Carum copticum* essential oil (CEO) loaded chitosan nanoparticles. *Int. J. Biol. Macromol.* **2015**, *81*, 283-290, https://doi.org/10.1016/j.ijbiomac.2015.08.010.
14. Cappello, G.; Spezzaferro, M.; Grossi, L.; Manzoli, L.; Marzio, L. Peppermint oil (Mintoil) in the treatment of irritable bowel syndrome: a prospective double blind placebo-controlled randomized trial. *Dig. Liver Dis.* **2007**, *39*, 530-536, https://doi.org/10.1016/j.dld.2007.02.006.
15. Mahboubi, M. Mentha spicata as natural analgesia for treatment of pain in osteoarthritis patients. *Complement. Ther. Clin. Pract.* **2017**, *26*, 1-4, https://doi.org/10.1016/j.ctcp.2016.11.001.
16. Manosroi, J.; Dhumtanom, P.; Manosroi, A. Antiproliferative activity of essential oil extracted from Thai medicinal plants on KB and P388 cell lines. *Cancer Letter* **2006**, *235*, 114-120, https://doi.org/10.1016/j.canlet.2005.04.021.
17. Hussain, A.I.; Anwar, F.; Nigam, P.S.; Ashraf, M.; Gilani, A.H. Seasonal variation in content, chemical composition and antimicrobial and cytotoxic activities of essential oils from four Mentha species. *J. Sci. Food Agric.* **2010**, *90*, 1827-1836, https://doi.org/10.1002/jsfa.4021.
18. Hajighasemi, F.; Khoshzaban, F. Cytotoxic effect of Mentha spicata aqueous extract on cancerous cell lines in vitro. *Journal of Medicinal Plants Research* **2011**, *5*, 5142-5147, https://doi.org/10.5897/JMPR.9000423.
19. Nedel, F.; Begnini, K.; Carvalho, P.H.d.A.; Lund, R.G.; Beira, F.T.; Del Pino, F.A.B. Antiproliferative activity of flower hexane extract obtained from Mentha spicata associated with Mentha rotundifolia against the MCF7, KB, and NIH/3T3 cell lines. *J. Med. Food* **2012**, *15*, 955-958, https://doi.org/10.1089/jmf.2011.0340.
20. Bardaweel, S.K.; Bakchiche, B.; Alsalamat, H.A.; Rezzoug, M.; Gherib, A.; Flamini, G. Chemical composition, antioxidant, antimicrobial and Antiproliferative activities of essential oil of Mentha spicata L. (Lamiaceae) from Algerian Saharan atlas. *BMC Complement Altern Med* **2018**, *18*, 201, https://doi.org/10.1186/s12906-018-2274-x.
21. Kazemzadeh, M.; Yaghmaei, P.; Mohammadi, S. Analgesic and anti-inflammatory effects of Tanacetum balsamita essential oil and one of its major constituents (quercetin) in male rats. *Clinical Neurology and Neuro-Science* **2017**, *1*, 60-66, http://dx.doi.org/10.11648/j.cnn.20170103.17.
22. Lv, L.; Yang, N.; Cao, Y.; Dang, J.; Cheng, L.; El-Sheikh, M.A.; Zhang, Y. d-Carvone inhibits the JAK/STAT3 signaling pathway and induced the apoptotic cell death in the human gastric cancer AGS cells. *J. Biochem. Mol. Toxicol.* **2021**, *35* , e22746, https://doi.org/10.1002/jbt.22746.
23. Vinothkumar, R.; Nalini, N. Supplementation with D-carvone Induces Cytotoxicity and Mitochondrial-Mediated Apoptosis in Human Colon Cancer Cell Lines HT-29 and SW480. *IJPBA* **2013**, *4*, 502-510.
24. Patel, P.B.; Thakkar, V.R. L-carvone induces p53, caspase 3 mediated apoptosis and inhibits the migration of breast cancer cell lines. *Nutr. Cancer* **2014**, *66*, 453-462, https://doi.org/10.1080/01635581.2014.884230.
25. MoemenbellahFard, M.D.; Abdollahi, A.; Ghanbariasad, A.; Osanloo, M. Antibacterial and leishmanicidal activities of Syzygium aromaticum essential oil versus its major ingredient, eugenol. *Flavour and Fragrance Journal* **2020**, *35*, 534-540, https://doi.org/10.1002/ffj.3595.
26. Alipanah, H.; Farjam, M.; Zarenezhad, E.; Roozitalab, G.; Osanloo, M. Chitosan nanoparticles containing limonene and limonene-rich essential oils: potential phytotherapy agents for the treatment of melanoma and breast cancers. *BMC Complementary Medicine and Therapies* **2021**, *21*, 186, https://doi.org/10.1186/s12906-021-03362-7.
27. Abedinpour, N.; Ghanbariasad, A.; Taghinezhad, A.; Osanloo, M. Preparation of Nanoemulsions of Mentha piperita Essential Oil and Investigation of Their Cytotoxic Effect on Human Breast Cancer Lines. *BioNanoScience* **2021**, *11*, 428–436, https://doi.org/10.1007/s12668-021-00827-4.
28. Karikas, G.A. Anticancer and chemopreventing natural products: some biochemical and therapeutic aspects. *Journal of BUON* **2010**, *15*, 627-638.
29. Bisi-Johnson, M.A.; Obi, C.L.; Hattori, T.; Oshima, Y.; Li, S.; Kambizi, L.; Eloff, J.N.; Vasaikar, S.D. Evaluation of the antibacterial and anticancer activities of some South African medicinal plants. *BMC Complement Altern Med* **2011**, *11*, 1-5, https://doi.org/10.1186/1472-6882-11-14.
30. Alipanah, H.; Zareian, P. Anti-cancer properties of the methanol extract of Boswellia serrata gum resin: Cell proliferation arrest and inhibition of angiogenesis and metastasis in BALB/c mice breast cancer model. *Physiology and Pharmacology* **2018**, *22*, 183-194.
31. Pirmoradian, M.; Budamgunta, H.; Chingin, K.; Zhang, B.; Astorga-Wells, J.; Zubarev, R.A. Rapid and deep human proteome analysis by single-dimension shotgun proteomics. *Mol. Cell. Proteomics* **2013**, *12*, 3330-3338, https://doi.org/10.1074/mcp.o113.028787.

32. Maksimović-Ivanić, D.; Bulatović, M.; Edeler, D.; Bensing, C.; Golić, I.; Korać, A.; Kaluđerović, G.N.; Mijatović, S. The interaction between SBA-15 derivative loaded with $Ph_3Sn(CH_2)_6OH$ and human melanoma A375 cell line: uptake and stem phenotype loss. *Journal of Biological Inorganic Chemistry* **2019**, *24*, 223-234, https://doi.org/10.1007/s00775-019-01640-x.
33. Dai, X.; Cheng, H.; Bai, Z.; Li, J. Breast Cancer Cell Line Classification and Its Relevance with Breast Tumor Subtyping. *J. Cancer* **2017**, *8*, 3131-3141, https://doi.org/10.7150/jca.18457.
34. Hugo, H.J.; Gunasinghe, N.P.A.D.; Hollier, B.G.; Tanaka, T.; Blick, T.; Toh, A.; Hill, P.; Gilles, C.; Waltham, M.; Thompson, E.W. Epithelial requirement for in vitro proliferation and xenograft growth and metastasis of MDA-MB-468 human breast cancer cells: oncogenic rather than tumor-suppressive role of E-cadherin. *Breast Cancer Res.* **2017**, *19*, 86, https://doi.org/10.1186/s13058-017-0880-z.
35. Mohafrash, S.M.; Fallatah, S.A.; Farag, S.M.; Mossa, A-T.H. *Mentha spicata* essential oil nanoformulation and its larvicidal application against *Culex pipiens* and *Musca domestica*. *Industrial Crops and Products* **2020**, *157*, 112944, https://doi.org/10.1016/j.indcrop.2020.112944.
36. Shahbazi, Y. Application of carboxymethyl cellulose and chitosan coatings containing Mentha spicata essential oil in fresh strawberries. *Int. J. Biol. Macromol.* **2018**, *112*, 264-272, https://doi.org/10.1016/j.ijbiomac.2018.01.186.
37. Shahbazi, Y.; Shavisi, N. Chitosan Coatings Containing *Mentha spicata* Essential Oil and Zinc Oxide Nanoparticle for Shelf Life Extension of Rainbow Trout Fillets. *Journal of Aquatic Food Product Technology* **2018**, *27*, 986-997, https://doi.org/10.1080/10498850.2018.1518945.
38. Azizkhani, M.; Sodanlo, A. Antioxidant activity of *Eryngium campestre* L., *Froriepia subpinnata*, and *Mentha spicata* L. polyphenolic extracts nanocapsulated in chitosan and maltodextrin. *Journal of Food Processing and Preservation* **2021**, *45*, e15120, https://doi.org/10.1111/jfpp.15120.
39. Ahmad, B.; Shireen, F.; Bashir, S.; Khan, I.; Azam, S. Green synthesis, characterisation and biological evaluation of AgNPs using Agave americana, Mentha spicata and Mangifera indica aqueous leaves extract. *IET nanobiotechnology* **2016**, *10*, 281-287, https://doi.org/10.1049/iet-nbt.2015.0053.
40. Ashbaugh, H.S.; Paulaitis, M.E. Effect of Solute Size and Solute−Water Attractive Interactions on Hydration Water Structure around Hydrophobic Solutes. *J. Am. Chem. Soc.* **2001**, *123*, 10721-10728, https://doi.org/10.1021/ja016324k.
41. Carlsson, J.; Åqvist, J. Calculations of solute and solvent entropies from molecular dynamics simulations. *Phys. Chem. Chem. Phys.* **2006**, *8*, 5385-5395, https://doi.org/10.1039/B608486A.
42. Prakash, A.; Baskaran, R.; Paramasivam, N.; Vadivel, V. Essential oil based nanoemulsions to improve the microbial quality of minimally processed fruits and vegetables: A review. *Food Research International* **2018**, *111*, 509-523, https://doi.org/10.1016/j.foodres.2018.05.066.
43. Das, S.; Singh, V.K.; Dwivedy, A.K.; Chaudhari, A.K.; Deepika; Dubey, N.K. Nanostructured Pimpinella anisum essential oil as novel green food preservative against fungal infestation, aflatoxin B_1 contamination and deterioration of nutritional qualities. *Food Chem.* **2021**, *344*, 128574, https://doi.org/10.1016/j.foodchem.2020.128574.
44. Liu, Y.; Niu, T-S.; Zhang, L.; Yang, J-S. Review on nano-drugs. *Natural Science* **2010**, *2*, 41-48, http://dx.doi.org/10.4236/ns.2010.21006.
45. Havel, H.A. Where are the nanodrugs ? An industry perspective on development of drug products containing nanomaterials. *AAPS J.* **2016**, *18*, 1351-1353, https://doi.org/10.1208/s12248-016-9970-6.
46. Peng, F.; Setyawati, M.I.; Tee, J.K.; Ding, X.; Wang, J.; Nga, M.E.; Ho, H.K.; Leong, D.T. Nanoparticles promote *in vivo* breast cancer cell intravasation and extravasation by inducing endothelial leakiness. *Nature Nanotechnology* **2019**, *14*, 279-286, https://doi.org/10.1038/s41565-018-0356-z.
47. Dudhani, A.R.; Kosaraju, S.L. Bioadhesive chitosan nanoparticles: Preparation and characterization. *Carbohydrate Polymers* **2010**, *81*, 243-251, http://dx.doi.org/10.1016/j.carbpol.2010.02.026.
48. Pan, Y.; Li, Y-j.; Zhao, H-y.; Zheng, J-m.; Xu, H.; Wei, G.; Hao, J-s.; Cui, Fu-d. Bioadhesive polysaccharide in protein delivery system: chitosan nanoparticles improve the intestinal absorption of insulin *in vivo*. *Int. J. Pharm.* **2002**, *249*, 139-147, https://doi.org/10.1016/s0378-5173(02)00486-6.